Applied Catalysis A: General 453 (2013) 142–150

Contents lists available at SciVerse ScienceDirect

Applied Catalysis A: General

journal homepage: www.elsevier.com/locate/apcata

Silica/clay organo-heterostructures to promote polyethylene–clay nanocomposites by *in situ* polymerization

Paula A. Zapata[a,*], Carolina Belver[b,c], Raúl Quijada[d], Pilar Aranda[b,*], Eduardo Ruiz-Hitzky[b]

[a] Grupo Polímeros, Facultad de Química y Biología, Universidad Santiago de Chile, USACH, Casilla 40, Correo 33, Santiago, Chile
[b] Instituto de Ciencia de Materiales de Madrid, ICMM-CSIC, c/Sor Juana Inés de la Cruz 3, Madrid E-28049, Spain
[c] Facultad de Ciencias, Universidad Autónoma de Madrid, Cantoblanco, 28049 Madrid, Spain
[d] Departamento de Ingeniería Química y Biotecnología, Facultad de Ciencias Físicas y Matemáticas, Universidad de Chile, Centro para la Investigación Interdisciplinaria Avanzada en Ciencias de los Materiales (CIMAT), Chile

ARTICLE INFO

Article history:
Received 29 August 2012
Received in revised form
27 November 2012
Accepted 1 December 2012
Available online 26 December 2012

Keywords:
Metallocene catalysts
Clay-based heterostructures
Polymer–clay nanocomposites
Polyethylene
Support catalysts

ABSTRACT

Two clay organo-heterostructures have been prepared and employed as fillers and catalyst supports for the development of polyethylene–clay nanocomposites. The new silica–clay organo-heterostructures have been obtained from two organoclays modified with tetramethoxysilane. In contrast to related heterostructures reported previously the organic moieties are not removed by heating and their presence intends to confer hydrophobicity to the interlayer region of the clay, even after delamination by hydrolysis-polymerization of the alkoxysilane takes place. These organo-heterostructures were used for preparing clay–polyethylene nanocomposites by *in situ* polymerizations in which the organo-heterostructures were added together with the metallocene catalyst, and by using the silica–clay as support for the metallocene catalysts. The polymers formed when the organo-heterostructures were used as support for the catalyst have higher molecular weights than the standard polyethylene formed under homogeneous conditions. Moreover, the presence of the inorganic silica network developed in the interlayer region of the organoclay favours the existence of a larger organophilic region in which it is possible to accommodate both the catalyst and the monomer, and hence when the polymer grows in this environment it can assist in the exfoliation of the clay layers inside the polyethylene matrix. The polymer particle morphology improved with the presence of the clay in the polymerization. The molecular weight for support systems presented an increasing ca. 40% compared to neat PE, and by TEM it was found that the clay layers were well dispersed in the PE matrix.

1. Introduction

Layered clay silicates, mainly 2:1 phyllosilicates, are extensively used for many applications due to their structural and surface properties. Their high cation exchange capacities allow replacing the original cations localized in the interlayer by other compounds like organic cationic molecules. Many papers have reported the development of ion-exchange methodologies in order to increase the interlayer distance, to improve the clay properties and to allow thermodynamically favourable interactions with organic molecules [1–3]. Other important studies had been focussed on the inclusion of small particles of metal oxides into the clay by different pathways, getting the so called pillared clays that display technological properties such as high surface area and thermal stability. Different pillaring processes have been reported for improving the clay's properties and its catalytic applications [4,5]. The ICMM-CSIC group has recently introduced a novel methodology to incorporate an inorganic network in a previously prepared organoclay, based on the formation of a silica network from the hydrolysis and polycondensation of alkoxysilanes [6,7]. The main characteristic of this method, in comparison with others [8–10], is the spontaneous formation of a homogeneous gel, resulting in a solid in which the silicate layers were dispersed in a silica matrix [7]. The resulting materials showed a degree of delamination, yielding a porous silica/clay heterostructure once the organic matter is eliminated. These results are very interesting and here we intend to use this type of clay organo-heterostructures as support for active catalytic species in order to get optimum catalysts to produce polyolefins that incorporate delaminated clays as reinforcing nanofillers.

In comparison with conventional Ziegler–Natta catalysts, metallocene catalysts present uniform active sites and yield polyolefins with narrow molecular weight ranges. [11] Metallocene complexes allow modelling of the catalyst's molecular structure, and

* Corresponding authors. Tel.: +56 2 7181149.
E-mail addresses: paula.zapata@usach.cl (P.A. Zapata), aranda@icmm.csic.es (P. Aranda).

0926-860X/$ – see front matter © 2012 Elsevier B.V. All rights reserved.
http://dx.doi.org/10.1016/j.apcata.2012.12.012

combined with methylaluminoxane as cocatalyst (MAO) they achieve high activity [12]. Nevertheless, homogeneous metallocenes present several disadvantages, such as difficulty to control polymer morphology (generating low density polymers), or reactor fouling and consequently not allowing them to be used in industrial polymerization processes. In order to overcome these problems found in homogeneous system, the metallocene catalysts have been immobilized on different inorganic surfaces [13,14] with the incorporation of nanoparticles in the polymerization [15]. Two methods can be used to obtain the *in situ* nanocomposite. The first route consists in the direct synthesis of the PE in the presence of the nanoparticles, with the nanoparticles placed in contact with the catalytic system (metallocene catalyst/MAO). The second route is the prior fixation of the catalytic system on the surface of the nanoparticle acting as support [16].

Clay particles have been used as support for metallocene catalysts by the *in situ* polymerization method, which consists in placing the monomer and the catalyst between the clay layers where the polymerization occurs [17,18]. As polymerization progresses, the spacing between the clay layers increases gradually and the dispersion state of the clays changes from intercalated to exfoliated, thus the clay can be distributed and gives rise to polymer–clay nanocomposites [19,20]. In this field diverse contributions related to the preparation of polypropylene (PP) and polyethylene (PE) nanocomposites by *in situ* polymerization using metallocene and Ziegler–Natta catalysts supported on montmorillonite clay minerals (MMT) have been reported, including clays modified with alkyammonium [21,22], alkylimidazolium and alkylpyridium [23,24,27] species, glycinate hydrochloride [25], stearyltrimethyl ammonium chloride (SAC) [26] and organosilanes (*e.g.* inopropyltriethoxysilane) [27]. In our group we have contributed to this field and observed that montmorillonite modified with octadecylamine (O–Clo) used as support for metallocene complexes or as filler (clay added directly into the reactor) shows catalytic activity comparable to neat polymer without clay, and the presence of the intercalated polymer clay phase with a few exfoliated silica particles was found by TEM [28]. Other studies have shown that the use of modified clay previously treated with MAO permitted getting better coordination of metallocene catalysts that allows optimum insertion of the monomer, resulting in nanocomposites with good dispersion of the clay in the polymer matrix [22,29]. In other approaches, like the one reported by Wei and coworkers [18], the metallocene is supported on a montmorillonite (MMT)/silica hybrid prepared by depositing silica nanoparticles between the interlayer of MMT by a sol–gel method. The catalytic activity decreases considerably compared to polymerization of neat PE, but the inorganic nanoparticles show good dispersion in the polyethylene matrix with exfoliated clay nanoparticles.

In the present work we intend to combine the advantages observed for silica–clay systems with our previous observations in the development of polyethylene–clay nanocomposites using silica–clay organo-heterostructures and applying the method developed by the ICMM-CSIC group [6,7]. Use of these materials as fillers and as supports of the metallocene catalyst promotes not only intercalation but also exfoliation of the silicate particles. In this way, we have prepared and used these materials as supports for the metallocene catalyst, trying to achieve optimum heterogeneous catalysts for polyolefin synthesis. The novelty here is that the silica nanoparticles are generated from a silicon-alkoxide previously intercalated in the interlayer region of an organoclay. Once the silica matrix is generated in a sol–gel process [6,7], it causes the expansion of the interlayer space of the clay while retaining the organophilic character of the interlayer region. Since in the present case the resulting clay organo-heterostructure was not subjected to calcination, it preserves the organophilicity and its ability to still make possible a further expansion of the stacked clay nanosheets. For the sake of comparison, the catalytic activity of these novel systems and the properties of the polyethylene were studied in comparison to systems prepared without clay. The dispersion of the modified clay in the polymer matrix and the final particle polymer morphology were also evaluated.

2. Experimental

2.1. Materials

A commercial sodium montmorillonite known as Cloisite®-Na (Na–Clo) supplied by Southern Clay with a cation exchange capacity (CEC) of 93 meq/100 g, was used to prepare the two organoclay derivatives by treatment with octadecylamine (ODA) and cetyltrimethylammonium bromide (CTAB) (90% and 96% purity, respectively, both from Aldrich). The silica–clay organo-heterostructures were prepared using 98% purity tetramethoxysilane (TMOS) (Aldrich) as silica source. The metallocenebis (*n*-butylcyclopentadienyl) zirconium dichloride ($(n\text{BuCp})_2\text{ZrCl}_2$, Aldrich) and methylaluminoxane (MAO) were chosen respectively as catalyst and co-catalyst for ethylene polymerization. Ethylene monomer was deoxygenated and dried by passing through columns of Cu catalyst (BASF) and activated molecular sieve (13X), respectively. Toluene solvent was purified by refluxing, and it was freshly distilled under nitrogen from a Na/benzophenone system. All manipulations during catalyst supporting and polymerization were carried out under an inert nitrogen atmosphere using the Schlenk technique.

2.1.1. Organoclay preparation

Modification of Na–Clo with ODA was carried out as previously described [28,30]. Octadecylamine (ODA), 1.6 g, was dissolved in a 50:50 v/v water:ethanol mixture acidified with HCl at 70 °C (pH 3.5), its dispersion was dropped on 5 g of Na–Clo dispersed in 500 mL of water and stirred vigorously for 2 h at 25 °C. The organically modified clay (O–Clo) was recovered by filtration and copiously washed with ethanol and water. The final solid was named O–Clo and corresponds to the octadecylamine organoclay in which the amino group is protonated and therefore compensates the silicate charge [2]. The ion-exchange reaction with CTAB to obtain the CTAB–Clo organoclay was also carried out by a previously described procedure [7]. In this case, 1 g of Na–Clo was dispersed in distilled water (100 mL) at 80 °C and stirred until a homogeneous dispersion was obtained. Then the CTAB solution was slowly added to reach twice the exchange capacity of the clay (93 meq/100 g). After stirring the mixture for 2 h at 80 °C the resulting solid was centrifuged and washed repeatedly with double-distilled water to remove the surfactant excess, and then dried at 100 °C for 12 h.

2.1.2. Preparation of silica–clay organo-heterostructures

The freshly prepared organoclays (O–Clo and CTAB–Clo) were dispersed in isopropyl alcohol (10% w/w ratio), increasing the dispersion with consecutive sonication treatments at 25 °C for 5 min and stirring for 12 h. Then TMOS was dropped on the suspension to produce a TMOS:organoclay w/w ratio of 2:1 and was stirred for 30 min to ensure its incorporation in the organophilic region of the organoclay. Then the stoichiometric amount of water mixed with isopropanol in a 2:1 H_2O:alcohol ratio to produce the hydrolysis of the four methoxy groups of the incorporated TMOS was added to the mixture. The hydrolysis–polycondensation process was performed at 50 °C with stirring and the final point was reached when a sudden sol–gel transition occurred in the medium after 4 and 6 h for O–Clo and CTAB–Clo, respectively. The recovered solid was dried at 50 °C, getting the final silica–clay organo-heterostructures

derived from O–Clo and CTAB–Clo, namely O–CloTMOS and CTAB–CloTMOS, respectively.

2.1.3. Incorporation of the metallocene catalyst in the silica–clay heterostructures

The O–CloTMOS and CTAB–CloTMOS organo-heterostructures were dried in vacuum at 120 °C for 24 h prior to the incorporation of the metallocene catalyst. Then 1 g of the clay organo-heterostructure was placed in contact with a toluene solution of $(n\text{BuCp})_2ZrCl_2$ and stirred for 8 h at 60 °C. The mixture was filtered through fritted glass and the solid was washed several times with toluene at 60 °C to remove excess reactant. The solid was then dried for 8 h in vacuum at room temperature. The effect caused by the concentration of metallocene solution on the amount of zirconium fixed on the final solid support was studied in the range of 0.73–2.92 mmol L^{-1} g^{-1} of clay organo-heterostructure. The percent Zr fixed in the clay was measured by ICP.

2.2. Polymerization reactions

2.2.1. Homogeneous ethylene polymerization

Polymerization reactions were carried out in a 600 mL glass reactor (Parr) equipped with mechanical stirring and temperature control. The homogeneous polymerization reactions were carried out by adding the MAO and metallocene catalyst solutions, allowing the ethylene monomer to enter the reactor. In each experiment 3×10^{-6} mol of metallocene catalyst in toluene was added to the reactor, using an amount of soluble MAO in an Al/Zr = 1400 mole ratio. The final volume of the solution in the reactor was 240 mL. Polymerization reactions were carried out at 60 °C and under 2 bar of ethylene pressure for 30 min with stirring at 1000 rpm. The polymerization was stopped by quenching with acidified (HCl) methanol (20 mL). The product was recovered by filtration, washed with ethanol and acetone, and dried overnight at room temperature. Catalytic activity was expressed as the mass of PE produced per unit time per mol of Zr and per unit pressure (kg mol^{-1} bar^{-1} h^{-1}). All the polymerization reactions were repeated twice to verify reproducibility.

2.2.2. Ethylene polymerization in the presence of the silica–clay organo-heterostructures (unsupported catalysts)

Ethylene polymerization in the presence of the silica–clay organo-heterostructures was performed by first adding 180 mL of toluene and 2.6 mL of MAO solution to the reactor, and then mixing with the metallocene solution (3×10^{-6} mol) for 2 min. A suspension of the silica–clay organo-heterostructure in toluene was then added, mixed for 2 min, and finally saturated with ethylene. In the present case the added amounts of the clay organo-heterostructure were chosen to be 1 and 5 wt% with respect to the weight of the standard polymerization product.

2.2.3. Ethylene polymerization in the presence of the silica–clay organo-heterostructures incorporating metallocene catalysts (supported catalysts)

This procedure is based on the method previously reported by our group, with montmorillonite modified with ODA (O–Clo) or nanosilica used as support for the metallocene catalysts [15,28,31]. The heterogeneous polymerization was carried out by first adding the MAO, followed by the organo clay-supported catalyst, mixing for 5 min, and finally saturating with ethylene for 30 min. The amount of metallocene, MAO, solvent, and operating conditions were the same as those used in the homogeneous polymerization.

2.3. Characterization techniques

2.3.1. Characterization of silica–clay organo-heterostructures and related materials

The structural properties of the raw and derivative clays were analyzed by powder X-ray diffraction (PXRD) on a Bruker D8 Diffractometer with a Sol-X energy dispersive detector, working at 40 kV and 30 mA and employing Cu Kλ filtered radiation. The diffractograms were registered between 2 and 70° (2θ) with a scanning velocity of 1.5°/min.

^{29}Si solid-state CP/MAS-NMR spectra were produced on a Bruker AV-400-WB spectrometer equipped with a 4 mm MASNMR probe, with the samples spinning at a rate of approximately 10 kHz. The operating frequency was 20 kHz, using 5 μs excitation pulses ($\pi/2$), recycle delays of 5 s, and 2048 scans. The chemical shifts of ^{29}Si resonances were evaluated in relation to kaolin (−91.5 ppm) and tetramethylsilane (TMS) as secondary and primary references, respectively.

FT–R spectra were recorded between 4000 and 400 cm^{-1} on a Perkin-Elmer 1730 Infrared Fourier Transform spectrometer, using the KBr pellet technique (about 1 mg of sample and 300 mg of dry KBr were used to prepare the pellets).

Characterization by Field Emission Scanning Electron Microscopy (FE-SEM) was performed on a NOVA NANOSEM model 230 FEI microscope that allows visualization of samples with various detectors and without the need of covering with a conductive coating.

Surface properties were analyzed by N_2 adsorption/desorption experiments performed at −196 °C on a static volumetric apparatus, Micromeritics ASAP 2010 analyzer. Prior to the analysis the samples (150–200 mg) were outgassed for 16 h at 120 °C. The specific surface area was calculated using the Brunauer–Emmett–Teller (BET) method [32–34]. The external surface area and micropore volume were obtained by means of the t-plot according to De Boer's method [35]. Total pore volume (Vp) of the solids was estimated from the amount of nitrogen adsorbed at a relative pressure of 0.99 [36]. Pore size distributions of microporous and mesoporous regions were performed using the Horvath–Kawazoe method [37] and the Barrett–Joyner–Halenda (BJH) method [38], respectively.

The Zr content of the supported catalysts was determined by inductively coupled plasma-atomic emission spectroscopy (ICP-AES) on a Perkin Elmer P-400 instrument.

2.3.2. Characterization of polymer derivatives

Molecular weight distributions of the polyethylene products were determined using a Waters Alliance GPC 2000 equipped with three Styragel HT-type columns (HT3, HT5, and HT6E). 1,2,4-Trichlorobenzene was used as solvent, at a flow rate of 1 cm^3 min^{-1} and a temperature of 135 °C. The columns were calibrated with polystyrene standards.

The melting temperature and enthalpy of fusion of the neat and nanocomposite PE samples were measured by differential scanning calorimetry (DSC) on a TA Instruments DSC 2920. The samples were heated from 25 °C to 180 °C and cooled to 25 °C at a rate of 10 °C min^{-1}; the values were taken from the second heating curve to eliminate any thermal history. Percent crystallinity was calculated using the enthalpy of fusion of an ideal polyethylene having 100% crystallinity (289 J g^{-1}) as reference [18].

Polymer particle morphology was observed by SEM on a LEO Gemini 1530 microscope. The dispersion of the clay in the composites was analyzed by TEM on a JOEL JEM-1200EXII microscope operating at 200 kV. Ultra-thin polyethylene nanocomposite specimens with a thickness of *ca.* 80 nm were cut with glass and diamond blades in an ultra-microtome (Sorvall MT 5000) at −40 °C.

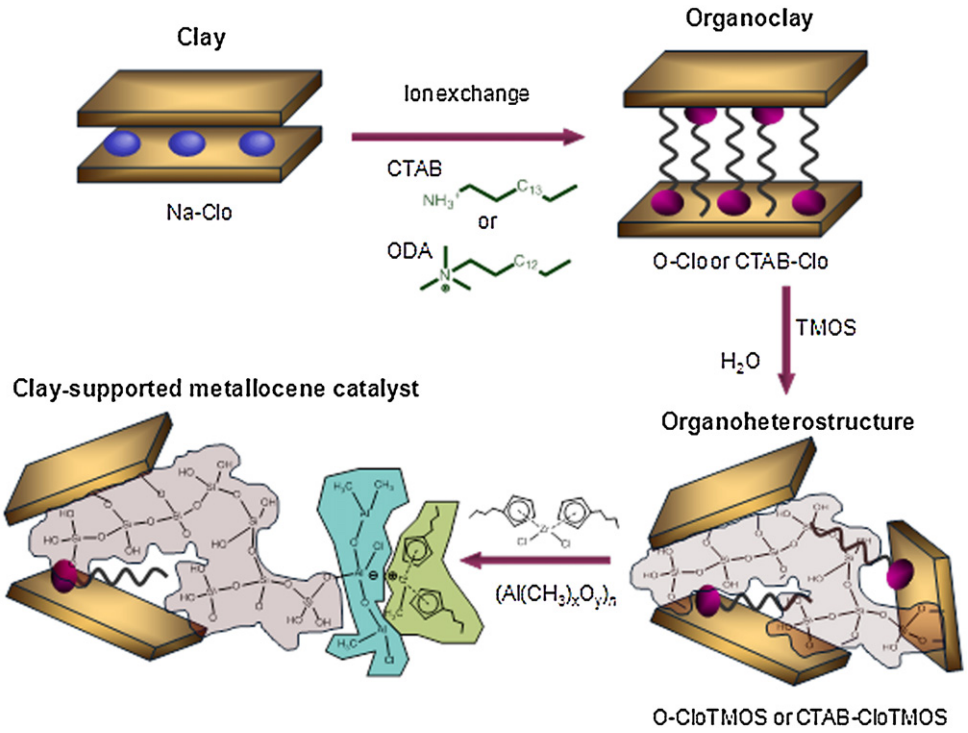

Fig. 1. Schematic representation of the preparation process of the silica–clay organo-heterostructure and the derived supported catalysts.

3. 3.Results and discussion

3.1. Silica–clay organo-heterostructures

The method used to prepare the silica–clay organo-heterostructures (Fig. 1) is based on a procedure previously developed for the preparation of silica–clay nanocomposites [6,7] but in the present case the samples were not submitted to the calcination step to preserve the organocations. Therefore, once dried the resulting organo-heterostuctures can be employed as support for the metallocene catalyst, as described in Fig. 1.

A basal spacing of 1.2 nm typical of Na-exchanged montmorillonites was determined from the XRD pattern of the pristine Na–Clo clay (Fig. 2). This basal spacing increases to 1.8 nm and 1.7 nm for O–Clo and CTAB–Clo organoclays, respectively. The results confirm that the clays were organic modified and organocations derived from ODA and CTAB have been successfully intercalated between the clay layers [28]. The later generation of the silica network in the interlayer region of the organoclays causes changes in the patterns, with the (0 0 1) diffraction peak in both cases of lower intensity and shifted to lower 2θ angles with respect to the starting organoclay, similar to that reported when other organo clays were used [3]. The O–CloTMOS organo-heterostructure shows a basal spacing of 1.9 nm with a slight reduction of the (0 0 1) peak intensity, indicating that the generated silica network is formed in the interlayer region and causes a loss of the crystal arrangement. In the case of the CTAB–CloTMOS organo-heterostructure the (0 0 1) reflection is very weak (Fig. 2e), which can be related to a greater loss of the silicate sheets stacking along the c-direction, which may be associated with a partial exfoliation of the clay layers. These results indicate that in the present clay organo-heterostructures the silicon alkoxide has also gone into the interlayer clay region of the organoclay, with its hydrolysis and polycondensation occurring between the layers and yielding highly disordered and even delaminated clay layers. Hence, as schematized in Fig. 2 the resulting materials can be described as organo-heterostructure composed of organoclay lamellae highly dispersed in the generated silica oxyhydroxide matrix.

The incorporation and creation of a silica oxyhydroxide matrix in the organoclay was also analyzed by solid-state ^{29}Si NMR spectroscopy (Fig. 3). From the analysis of the relative intensity of the Q^n signals, (where n can be 1, 2, 3, 4, and denotes the number of SiO units bonded to a Si atom), it is possible to get an idea of the degree of hydrolysis and condensation of the intercalated alkoxide precursor. As expected, the spectra of the O–Clo and CTAB–Clo organo clays (Fig. 3) show a signal at 94 ppm typical of these silicates, presenting Si atoms in tetrahedral coordination, forming $[Si(OSi)_3OAl]$ structural environments [39,40], confirming that the alkylammonium cation intercalation does not modify the structural

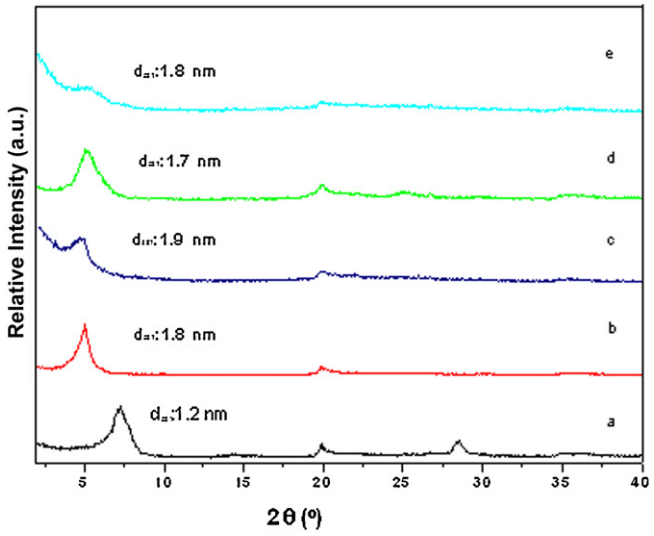

Fig. 2. XRD patterns of the starting clay: (a) Na–Clo and various of its related derivatives, (b) O–Clo, (c) O–CloTMOS, (d) CTAB–Clo and (e) CTAB–CloTMOS.

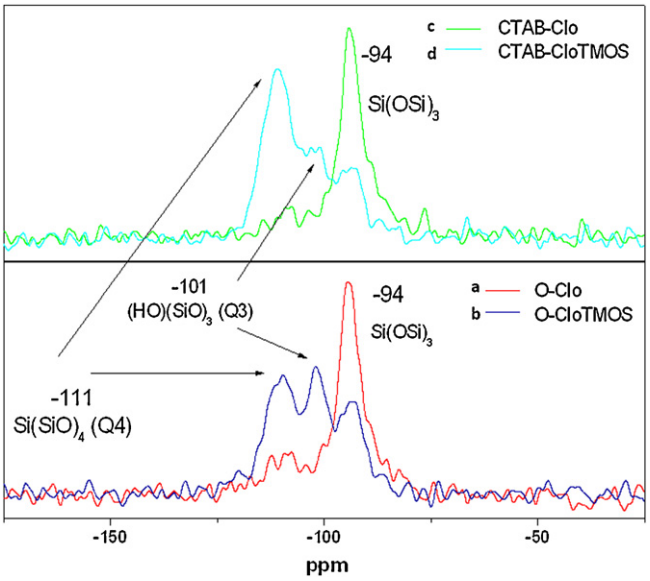

Fig. 3. ^{29}Si NMR solid state spectra of the modified forms: (a) O–Clo, (b) O–CloTMOS, (c) CTAB–Clo, and (d) CTAB–CloTMOS.

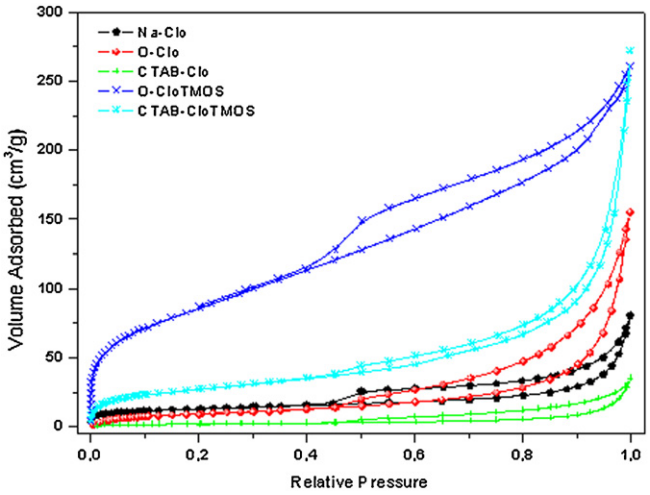

Fig. 5. N_2 adsorption–desorption isotherms of: –O–Clo, –O–CloTMOS, –CTAB–Clo and –CTAB–CloTMOS.

environments of the silicate sheets. However, the spectra of the organo-heterostructures show quite different profiles. The spectrum of O–CloTMOS displays two new signals centred at *ca.* 101 and 110 ppm and does not show the characteristic signal of the silicon precursor(TMOS) located at −78.5 ppm [41], which confirms the practically complete polycondensation of the silica precursor. The peaks at 101 and 111 ppm can be assigned to Q^3 and Q^4 signals related to Si atoms in $(HO)(SiO)_3$ and $Si(SiO)_4$ environments, respectively, generated from the polycondensation of TMOS [42,43]. The degree of polycondensation of the generated polysiloxane is defined as a relation between Q^4/Q^3, which is calculated by deconvolutions of the ^{29}Si NMR spectrum. The results obtained for the O–CloTMOS and CTAB–CloTMOS were Q^4/Q^3: 2.2 and 3.2, respectively, which indicates a higher degree of polycondensation for the CTAB–CloTMOS heterostructures and greater incorporation of the silica.

The FTIR spectrum of pristine Na–Clo shows the characteristic vibration modes of this type of 2:1 layered silicates (Fig. 4a), with the bands associated with the OH stretching vibration modes of

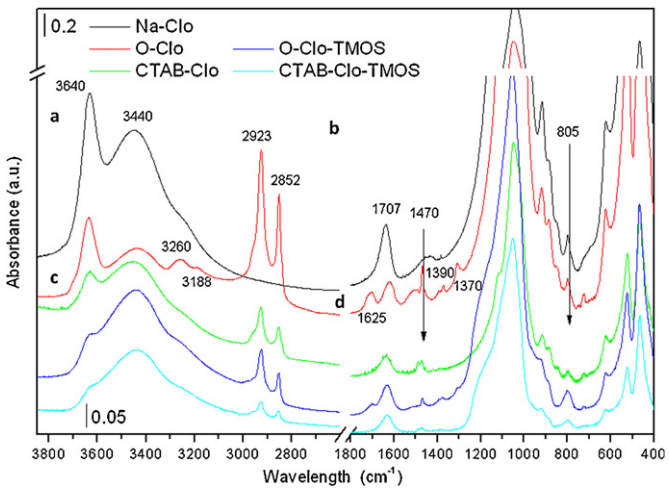

Fig. 4. FT–IR spectra of: (a and b) the pristine clay and the organoclays at different wavenumber values (a) 3850–2600 cm^{-1}, (b) 1800–1200 cm^{-1}, (c and d) the organo-heterostructures compared to the corresponding organoclays.

OH–Al bonds and water molecules at 3630 and 3440 cm^{-1}, respectively, the water bending mode at 1625 cm^{-1}, the Si–O stretching mode of the silicate network in the 1100–1050 cm^{-1} region, and the (Al_2OH) and (MgAlOH) deformations at 917 and 843 cm^{-1}, respectively [44]. In the spectra of the prepared organoclays (Fig. 4b and c) there are additional bands at 2930 and 2854 cm^{-1} as well as at about 1472 cm^{-1} related to the stretching vibrations of CH_2 groups and to the bending of CH_3 and CH_2, respectively, of the intercalated alkylammonium species [45]. Additionally, in the spectrum of the O–Clo organoclay (Fig. 4c) additional bands are seen at 3260 and 3188 cm^{-1} as well as at 1707 and 1508 cm^{-1}, related to N–H stretching and bending vibration modes, respectively, together with a band at around 1300 $cm^{-1}$and at (?), related to C–N vibrations, all of them due to the presence of the terminal amine group of the octadecylamine ion. The formation of the polysiloxane matrix in the organo-heterostructures can be inferred from the differences between the corresponding spectra (Fig. 4) with those of the starting organoclays. The presence of the bands related to the alkyl chains (in the 2900 and 1470 cm^{-1} regions) in those spectra indicates that in the process the organocations are preserved in these systems. The presence of these organic moieties of organophilic nature will be useful to attain the incorporation of the metallocene catalyst. The main changes are observed in the region of the Si–stretching vibration modes. In both heterostructures the spectra show that in the characteristic band at around 1050 cm^{-1} there is also a shoulder defined at around 1200 cm^{-1}. A new band is also defined at 805 cm^{-1} that can be ascribed to Si–O vibrations of tetrahedral SiO_4. In both cases these new bands are clearly related to the presence of the generated polysiloxane matrix.

The effect caused by the organic modifications on the textural properties of the Na–Clo montmorillonite was evaluated by the corresponding nitrogen adsorption–desorption isotherms at 77 K, shown in Fig. 5. The isotherms of the organoclays are classified as type II with a type H3 hysteresis loop, called type IIb by Rouquerol et al. [34]. Type IIb isotherms are usually obtained for solids with aggregates of plate-like particles and non-rigid slit-shaped pores. The silica matrix generated in the organo-heterostructures increases the volume of adsorbed nitrogen and provokes a textural modification of the O–Clo heterostructure. The curve described by the O–CloTMOS organo-heterostructure is quite different from the others, classified as mixed type I and IIb. The amount of nitrogen adsorbed at low relative pressures (<0.05) is quite high and indicates the creation of microporosity mainly caused by

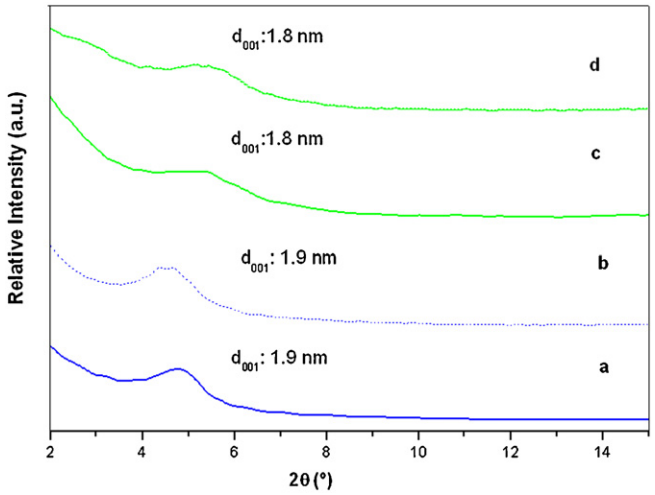

Fig. 6. XRD patterns of: (a) O–CloTMOS, (b) Cat/O–CloTMOS, (c) CTAB–CloTMOS and (d) Cat/CTAB–CloTMOS.

the presence of a polysiloxane matrix intercalated in the organoclay.

The textural properties derived from N_2 isotherms are collected in Table 1, calculated by the classical theories indicated in the experimental section. The organoclays present low specific surface areas, even lower than those of pristine montmorillonite in the case of CTAB–Clo. This is due to the blocking of nitrogen molecules from the pore network caused by the presence of organic moieties, with higher steric effect when using CTAB instead of ODA, probably due to its ternary nature [46]. The organo-heterostructures have higher specific surface areas, the highest of which is that of the O–CloTMOS organo-heterostructure. This improvement of the surface area may be related to the additional surface and porosity provided by the polysiloxane matrix generated after the polycondensation of the alkoxide precursor. The micro- and mesoporosity of the samples also has an effect, as shown clearly by the pore volume, thereby showing an improvement of the textural properties compared to the pristine montmorillonite.

3.2. Characterization of the clay-supported metallocene catalysts

The prepared CTAB–CloTMOS and O–CloTMOS organo-heterostructures were used to incorporate the $(n\text{BuCp})_2ZrCl_2$ catalyst by direct adsorption of the metallocene in a toluene solution to Cat/O–CloTMOS and Cat/CTAB–CloTMOS. The XRD patterns of the resulting Cat–O–CloTMOS and Cat–CTBA–CloTMOS materials show slight differences with respect to the starting organo-heterostructures (Fig. 6). The metallocene complex had an average size of 0.8 nm [47] and it may be assumed that it can be accommodated in the organophilic region of the organo-heterostructures, which become easily accessible considering the high disorganization in the silicate layer stacking provoked by the incorporation of the polysiloxane network. It is expected that in the present case and due to the larger surface area and microporosity of the organo-heterostructures compared to the starting organoclays, these regions were more accessible to accommodate the catalyst compared to other clay substrates reported previously [28]. The metallocene incorporation in the interlayer clay was also verified by indirect measurement of the Zr content by ICP (Table 3).

3.3. PE–clay nanocomposites

3.3.1. Ethylene polymerization in the presence of the silica–clay organo-heterostructures (unsupported catalysts)

In a first set of experiments the characteristics of polyethylene nanocomposites prepared by homogeneous polymerization of ethylene carried out with the metallocene complex in solution in the presence of the CTAB–CloTMOS and O–CloTMOS organo-heterostructures and compared to those of materials resulting when using unmodified Na–Clo were tested (Table 2) [28]. When the O–CloTMOS system (1 wt% of clay) was used as filler in the polyethylene synthesis reaction, the catalytic activity increases slightly (in terms of $kg\,mol^{-1}\,h^{-1}\,bar^{-1}$) with respect to the homogeneous reaction without any filler; similar results were also reported for Na–Clo/PE-based nanocomposites. Therefore, this catalytic performance can also be attributed to the behaviour of the clay particles as spacer centres, hindering the bimolecular deactivation between neighbouring zirconocenes in the solutions [28]. When CTAB–CloTMOS was used as filler the catalytic activity decreased slightly compared to that of neat PE (Table 2). With regard to the properties of the polymer, its molecular weight remains without significant changes compared to the synthesis reaction with and without fillers and with a PDI of 2.0 characteristic of metallocene catalysts. It should also be noted that the percentage of crystallinity decreases slightly in the clay organoheterostructure/PE nanocomposites compared to neat PE, indicating that the incorporation of the particles reduces slightly the degree of the crystallinity. The same results were found for PE/silica and PE/silver nanocomposites [48,49].

3.3.2. Ethylene polymerization in the presence of silica–clay organo-heterostructures incorporating metallocene catalysts (supported catalysts)

In a second set of experiments PE was polymerized using clay-based compounds in order to immobilize the metallocene complex catalyst (Table 3).

Catalytic activity parameters for ethylene polymerization using Cat/O–CloTMOS are quite similar to those found in the homogenous catalyzed reaction, in particular with low amounts of zirconium. In general, when metallocenes have been supported on clay or silica, there is a loss of activity [50]. But these supported systems have a very interesting behaviour that may be related to the textural properties (high surface area and porosity) of the O–CloTMOS system, which facilitate access of the reactive species to the catalytic active centres. It is concluded that the activity of these supported systems is comparable to that of the homogeneous systems. These high activity values using the heterostructures as support can be explained assuming that the supports presented a good dispersion of the active site, and therefore good polymerization activity [12,36,51]. The Cat/CTAB–CloTMOS catalytic system showed lower activities than for neat PE. This behaviour may be related to difficulties in the access of reagents to the active sites or it can be due to this heterostructure undergoing high condensation, and therefore there is a high population of hydroxyl groups that can deactivate the metallocene catalyst. When Tables 2 and 3 are compared, the catalytic activity of O–CloTMOS used as filler (unsupported catalyst) or as support for metallocene catalysts is similar. This can be due to the fact that the high surface area of the clay allows the fixation of metallocene catalysts on the layer. On the other hand, the catalytic activity when Na–Clo was used as support decreased with respect to the unsupported catalyst system. The catalytic activity may decrease due to deactivation reactions with neighbouring hydroxyl groups on the clay's surface or as a consequence of the fixation of the metallocene on less accessible sites in the clay structure [28].

Table 1
Textural properties of different samples.

Sample	S_{BET} [a] (m^2/g)	S_{MP} [b] (m^2/g)	S_{EXT} [c] (m^2/g)	V_{MP} [d] (cm^3/g)	V_t [e] (cm^3/g)	V_{BJH} [f] (cm^3/g)
Na–Clo	36	9	27	0.0081	0.1249	0.1091
O–Clo	36	–	36	–	0.2403	0.1943
O–CloTMOS	301	14	287	0.0090	0.4036	0.3520
CTAB–Clo	8	–	8	–	0.0547	0.0451
CTAB–CloTMOS	98	7	91	0.0018	0.4196	0.3257

[a] Specific surface area determined by the BET method.
[b] External surface area by the t-method.
[c] Micropore surface area by the t-method.
[d] Micropore volume by the t-method.
[e] Total volume calculated at maximum pressure from the adsorption branch.
[f] Mesopore volume data from the desorption branch by BJH analysis.

Table 2
Results of ethylene polymerization in the presence of silica–clay organo-heterostructures (unsupported catalysts).

Filler sample	Clay content (wt%)	Catalytic activity ($kg\,mol^{-1}\,h^{-1}\,bar^{-1}$)	M_w ($kg\,mol^{-1}$)	PDI	T_m (°C)	χ (%)
Neat PE without clay	0	3900	200	2.1	139	67
Na–Clo [28]	1	4800	164	2.0	137	70
O–CloTMOS	1	4200	190	2.0	136	62
O–CloTMOS	5	4000	–	–	136	63
CTAB–CloTMOS	1	3600	180	2.1	137	63
CTAB–CloTMOS	5	3900	–	–	136	60

Polymerization conditions: [Zr]: 3×10^{-6} mol; Al(MAO)/Zr: 1400; ethylene pressure: 2 bar; temperature: 60 °C; time: 0.5 h; solvent: 200 mL of toluene. T_m: melting point; M_w: molecular weight; PDI: M_w/M_n polydispersity; χ: percent crystallinity.

In the present case all the final PE-based nanocomposites show similar melting points compared to neat polyethylene. However, they present slightly lower crystallinity and higher molecular weight. The molecular weight increased *ca.* 40% with the supported system with respect to the material prepared without fillers. The formation of PE with higher molecular weight may be related to the decrease of transfer chains from β hydrogen [12]. It has been found that when the polymerization is carried out on metallocenes immobilized in a nanoscopic space, such as clay, the active species can be protected from other chemicals causing termination of polymer chain propagation [52]. The polydispersity (M_w/M_n) values are close to 2 in all cases, which is characteristic of polyethylene polymers produced with this type of metallocene catalysts.

Visual inspection of neat PE and the nanocomposites prepared with the supported metallocene catalysts (PE/Cat/OCloTMOS and PE Cat/CTABCloTMOS) shows that the former are composed of fibre-like particles, while the nanocomposites are clearly more powdery products. Observation of these materials by FE-SEM allows comparison of their morphologies (Fig. 7). The neat polymer presented a compact morphology, while the nanocomposites are formed by bundles of thin PE fibres which are disaggregated. This observation indicates that ethylene polymerization on these heterogeneous catalysts progresses in a different way, giving rise to PE with disaggregated morphology. The influence on the morphology of the polymer has been described in other metallocene catalysts supports like silica nanospheres [53,54], and the improvement of the morphology can be related to a good dispersion of the active sites. On the other hand, the visual aspect of the polymer changed in comparison with the polymer obtained without clay heterostructure. The improvement of the morphology yielded a fine powder. This point is very important for further industrial processes.

Nanocomposites were also characterized by TEM (Fig. 8). In the nanocomposite prepared under homogeneous conditions using 1 wt% of O–CloTMOS clay base as filler (Fig. 8a), exfoliated particles of O–CloTMOS are seen in the polyethylene matrix together with large amounts of non-exfoliated clay particles. On the other hand, when O–CloTMOS is incorporated directly into the reactor, it becomes more difficult for the catalytic systems to penetrate into the clay layer, the polymer in general grows around the clay, and therefore the dispersion of the clay is less than in supported systems, as shown in the TEM images (Fig. 8b).

In contrast, TEM images of PE/Cat/O–CloTMOS (1.7 wt%) (Fig. 8b) show the presence of exfoliated clay particles with a quite homogeneous distribution of the clay layers into the polymer matrix. PE/Cat/CTAB–CloTMOS nanocomposite images (Fig. 8c) show that in this case exfoliated and intercalated clay particles coexist. This result can be related to the fact that active centres in the support system based on Cat/O–CloTMOS are more accessible to ethylene monomers, favouring the growth of the polymer and allowing the disaggregation of the clay, yielding exfoliated clay particles well distributed in the PE matrix, This did not happen when O–Clo was used as support, as described in a previous report [28].

Table 3
Results of ethylene polymerization in the presence of silica–clay organo-heterostructures incorporating metallocene catalysts (supported catalysts).

Catalyst	Zr (%) (fixed)[a]	Clay content (%)	Catalytic activity ($kg\,mol^{-1}\,h^{-1}\,bar^{-1}$)	M_w ($kg\,mol^{-1}$)	PDI	T_m (°C)	χ (%)
Neat PE without clay	–	–	3900	200	2.14	139	67
Cat/Na–Clo [28]	0.1	1.8	2950	373	1.82	136	71
Cat/O–CloTMOS	0.1	1.7	4000	350	1.86	137	58
Cat/O–CloTMOS	0.4	0.6	3500	–	–	137	57
Cat/CTAB–CloTMOS	0.1	1.7	2500	340	1.87	138	58
Cat/CTAB–CloTMOS	0.4	0.6	2700	–	–	137	60

Polymerization conditions: [Zr]: 3×10^{-6} mol; Al(MAO)/Zr: 1400; ethylene pressure: 2 bar; temperature: 60 °C; time: 0.5 h; solvent: 200 mL of toluene.
[a] Zr (%) measured by ICP.

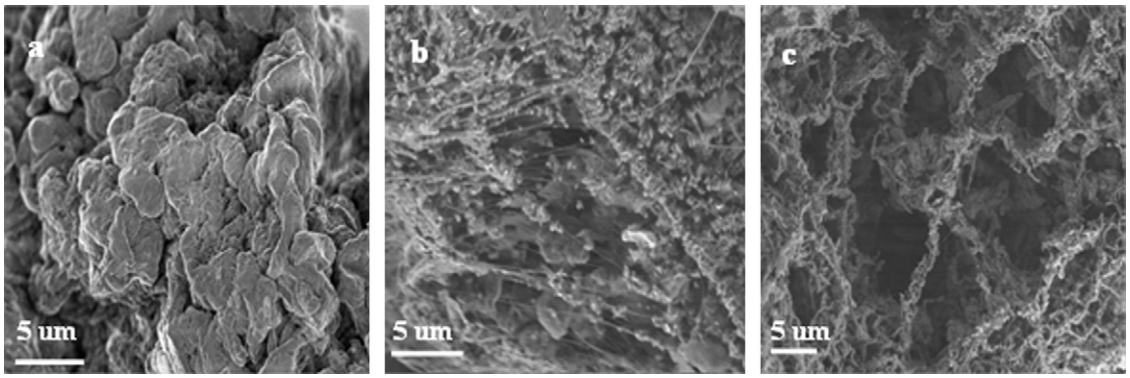

Fig. 7. FE-SEM images of neat PE (a) and PE/Cat/OCloTMOS (1.7 wt%) (b) and PE Cat/CTABCloTMOS (1.7 wt%) nanocomposites (c).

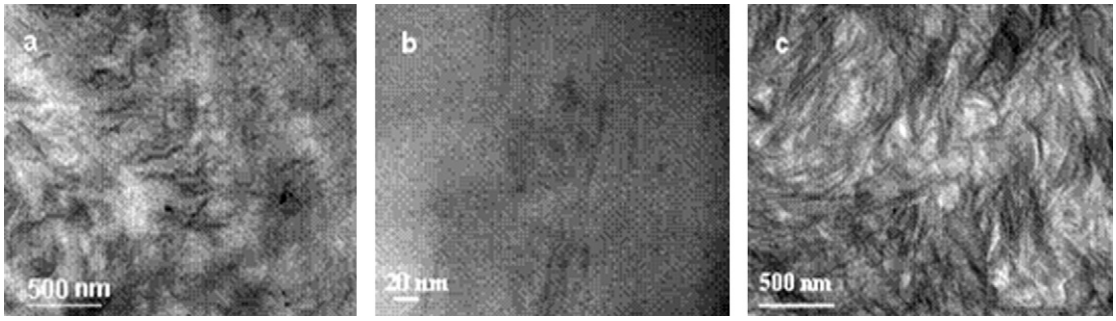

Fig. 8. TEM images of PE/O–CloTMOS (1 wt%) nanocomposite obtained using (a) O–CloTMOS as filler, (b) PE/Cat/O–CloTMOS, and (c) PE/Cat/CTAB–CloTMOS nanocomposites obtained with (1.7 wt%) O–CloTMOS and CTAB–CloTMOS supported catalysts, respectively.

4. Conclusions

A new support from organo-heterostructures clays, using a methodology based on the controlled hydrolysis of alcoxysilane into organoclay has been developed for fixing metallocene catalysts and for promoting ethylene polymerization.

The modification of organoclay by the incorporation of a siloxane network caused improved the textural properties of heterostructures. When O–CloTMOS was used as support it led to optimum dispersion of clay layers in the polymer matrix. This can be due to the fact that the O–CloTMOS clays allowed optimal fixation of the Zr catalysts and therefore the active centres were better dispersed, allowing polymer growth and delamination of the clay.

An improvement in polymer morphology and textural appearance of the polymer particles was achieved using the heterostructures as support for metallocene catalyts. The molecular weight of the polymers obtained with support systems increased *ca.* 40% compared to neat PE. These characteristics found in the polyethylene when support systems were used may help polymer processing in industry with respect to neat PE.

Acknowledgements

The authors acknowledge the financial support of CONICYT, Chile, under FONDECYT Project 1100058, and of CICYT, Spain, under Project MAT2009-09960. P. Zapata acknowledges the financial support of CONICYT under insertion project 79100010 and FONDECYT Project 11110237. Special thanks are due to Dr. Ingo Lieberwirth of the Max Planck Institute for Polymer Research, Mainz, Germany, for providing the TEM equipment, to Juan Benavides for helping in the polymer synthesis, and to Mr. Andres Valera (FE-SEM Unit, ICMM-CSIC) for assistance in sample characterization. C.B. is indebted to the MICINN for a Ramon y Cajal postdoctoral contract.

References

[1] F. Bergaya, B.K.G. Theng, G. Lagaly (Eds.), Handbook of Clay Science, Elsevier Science Ltd, Amsterdam, 2006.
[2] E. Ruiz-Hitzky, P. Aranda, M. Serratosa, in: S.M. Auerbach, K.A. Carrado, P.K. Dutta (Eds.), Organic/Polymeric Interactions with Clays Handbook of Layered Materials, Marcel Dekker, New York, 2004, pp. 91–154.
[3] E. Ruiz-Hitzky, P. Aranda, M. Darder, G. Rytwo, J. Mater. Chem. 20 (2010) 9306–9321.
[4] S. Korili, A. Gil, R. Trujillano, M.A. Vicente, Pillared Clays and Related Catalysts, Springer, New York, 2010.
[5] Nanoarchitectures Based on Clay Materials in Manipulation of Nanoscale Materials: An Introduction to Nanoarchitectonics, ed., Royal Society of Chemistry, 2012, pp. 87-105.
[6] S. Letaïef, M.A. Martín-Luengo, P. Aranda, E. Ruiz-Hitzky, Adv. Funct. Mater. 16 (2006) 401–409.
[7] S. Letaïef, E. Ruíz-Hitzky, Chem. Commun. 24 (2003) 2996–2997.
[8] M. Polverejan, T. Pauly, T. Pinnavaia, Chem. Mater. 12 (2000) 2698–2704.
[9] L. Baoshan, M. Huihui, L. Xiao, M. Wei, L. Zhenxing, J. Colloid Interface Sci. 336 (2009) 244–249.
[10] R. Ishii, M. Nakatsuji, K. Ooi, Microp. Mesop. Mater. 79 (2005) 111–119.
[11] D. Bianchini, F. Stedile, J. dos Santos, Appl. Catal. A Gen. 261 (2004) 57–67.
[12] J. dos Santos, C. Kruga, M. Barbosa, F. Chiarello, J. Duponta, M. de Camargo, J. Mol. Catal. A Chem. 139 (1999) 199–207.
[13] C. Covarrubias, R. Quijada, R. Rojas, Appl. Catal. A Gen. 347 (2008) 223–233.
[14] G. Hlatky, Chem. Rev. 100 (4) (2000) 1347–1376.
[15] P. Zapata, R. Quijada, R. Benavente, J. Appl. Polym. Sci. 119 (2011) 1771–1780.
[16] M. Ribeiro, A. Deffieux, M. Portela, Ind. Eng. Chem. Res. 36 (1997) 1224–1237.
[17] X. Jun-Ting, Z. Yan-Qin, Q. Wang, F. Zhi-Qiang, Polymer 46 (2005) 11978–11985.
[18] L. Wei, T. Tang, B. Huang, J. Polym. Sci. A Polym. Chem. 42 (2004) 941–949.
[19] Q. Wang, Z. Zhiyin, S. Lixin, X. Hong, L. Wang, J. Polym. Sci. A Polym. Chem. 42 (2004) 38–43.
[20] M. Alexandrea, Ph Duboisa, T. Sunb, J. Garcesb, R. Jérôme, Polymer 43 (2002) 2123–2132.
[21] J. Heinemann, P. Reichert, R. Thomann, R. Mülhaupt, Macromol. Rapid Commun. 20 (1999) 423–430.
[22] L. Dong-ho, K. Hyuk-soo, Y. Keun-byoung, M. Kyung Eun, S. Kwan, N. Seok Kyun, Sci. Technol. Adv. Mater. 6 (2005) 457–462.
[23] H. Aihua, H. Haiqing, H. Yingjuan, D. Jin-Yong, H. Charles, Macrom. Rapid Commun. 25 (2004) 2008–2013.

[24] H. Aihua, L. Wang, L. Junxing, D. Jinyong, H. Charles, Polymer 47 (2006) 1767–1771.
[25] Y. Huang, K. Yang, J. Dong, Macrom. Rapid Commun. 27 (2006) 1278–1283; Y. Xua, R. Liua, D. Wua, Y. Suna, H. Gaob, H. Yuanb, Fe. Deng, J. Non-Cryst. Solids 351 (2005) 2403–2413.
[26] J. Hwu, G. Jiang, J. Appl. Polym. Sci. 95 (2005) 1228–1236.
[27] C. Liu, T. Tang, B. Huang, J. Catal. 221 (2004) 162–169.
[28] P.A. Zapata, R. Quijada, C. Covarrubias, E. Moncada, J. Retuert, J. Appl. Polym. Sci. 113 (2009) 2368–2377.
[29] Y. Huang, K. Yang, J.-Y. Dong, Polymer 48 (2007) 4005–4014.
[30] E. Moncada, R. Quijada, J. Retuert. J. Appl. Polym. Sci. 103 (2007) 698–706.
[31] P.A. Zapata, R. Quijada, H. Palza, I. Lieberwirth, Appl. Catal. A Gen. 407 (2011) 181–187.
[32] P. Carrott, K. Sing, J.H. Raistrick, Colloids Surf. 21 (1986) 9–15.
[33] S. Brunauer, P.H. Emmett, E. Teller, J. Am. Soc. 60 (1983) 309–319.
[34] F. Rouquerol, J. Rouquerol, K. Sing, Adsorption by Powders and Porous Solids: Principles, Methodology and Applications, Academia Press, London, 1999.
[35] B.C. Lippens, J.H.d. Boer, J. Catal. 4 (1995) 319–323.
[36] S.J. Gregg, K. Sing, Adsorption, Surface Area and Porosity, Academic Press, London, 1982.
[37] G. Horvath, K. Kawazoe, J. Chem. Eng. Japan 16 (1983) 470–475.
[38] G.P. Barrett, L.G. Joyner, R.H. Halenda, J. Am. Chem. Soc. 73 (1951) 373–380.
[39] H. Hongping, D. Jannick, G. Jocelyne, G. Jean-François, J. Coll. Interface Sci. 288 (2005) 171–176.
[40] C. Belver, P. Aranda, M.A.Martín-Luengo, E. Ruiz-Hitzky, Microp. Mesop. Mater. 147 (2012) 157–166.
[41] J. Brinker, G. Scherer, The Physics and Chemistry of Sol–Gel Processing, ed. Academic Press, San Diego/New York/Boston, 1990.
[42] X. Yao, Li Ruili, W. Dong, S. Yuhan, G. Hongchang, Y. Hanzhen, D. Feng, J. Non-Cryst. Solids 351 (2005) 2403–2413.
[43] Z. Olejniczaka, M. Łęczkab, K. Cholewa-Kowalskab, K. Wojtachb, M. Rokitab, W. Mozgawa, J. Mol. Struct. 744-747 (2005) 465–547.
[44] J.T. Kloprogge, R.L. Frost, J. Colloid Interface Sci. 296 (2006) 640–646.
[45] Y. Xi, Q. Zhou, R.L. Frost, H. He, J. Colloid Interface Sci. 311 (2007) 347–353.
[46] F. Koolia, Y. Liub, S.F. Alshahateetc, M. Messalia, F. Bergaya, Appl. Clay Sci. 43 (2009) 357–363.
[47] H. Rahialaa, I. Beurroiesa, T. Eklunda, K. Hakalab, R. Gougeonc, P. Trensd, J.B. Rosenholm, J. Catal. 188 (1999) 14–23.
[48] K. Chrissafisa, K.M. Paraskevopolusa, E. Pavlidoua, D. Bikiaris, Thermochim Acta 458 (2009) 65–71.
[49] P.A. Zapata, L. Tamayo, M. Páez, E. Cerda, I. Azocar, F.M. Rabagliati, Eur. Polym. J. 47 (2011) 1541–1549.
[50] G. Griselda, M. Serefi, R. Guimaraes, J. Rohrmann, F. Stedile, J.H.Z. Dos Santos, J. Mol. Catal. A Chem. 189 (2002) 233-.
[51] J.C. Chien, R. Sugimoto, J. Polym. Sci. Polym. Chem. Ed. 29 (1991) 459.
[52] L. Cui, H. Cho, J. Shin, N. Tarte, Macromol. Symp. 260 (2007) 49–57.
[53] P.A. Zapata, R. Quijada, R. Benavente, I. Lieberwirth, Macromol. React. Eng. 5 (2011) 294–302.
[54] P.A. Zapata, Quijada R., J. Nanomater. (2012), doi:194543.